JOURNAL OF BACTERIOLOGY, Dec. 2008, p. 7918–7924 Vol. 190, No. 24
0021-9193/08/$08.00+0 doi:10.1128/JB.00911-08
Copyright © 2008, American Society for Microbiology. All Rights Reserved.

The *Mycobacterium avium* Complex *gtfTB* Gene Encodes a Glucosyltransferase Required for the Biosynthesis of Serovar 8-Specific Glycopeptidolipid[▽]

Yuji Miyamoto,[1]* Tetsu Mukai,[1] Yumi Maeda,[1] Masanori Kai,[1] Takashi Naka,[2] Ikuya Yano,[2] and Masahiko Makino[1]

Department of Microbiology, Leprosy Research Center, National Institute of Infectious Diseases, 4-2-1 Aobacho, Higashimurayama, Tokyo 189-0002, Japan,[1] and Japan BCG Central Laboratory, 3-1-5 Matsuyama, Kiyose, Tokyo 204-0022, Japan[2]

Received 2 July 2008/Accepted 29 September 2008

Mycobacterium avium **complex (MAC) is one of the most common opportunistic pathogens widely distributed in the natural environment. The 28 serovars of MAC are defined by variable oligosaccharide portions of glycopeptidolipids (GPLs) that are abundant on the surface of the cell envelope. These GPLs are also known to contribute to the virulence of MAC. Serovar 8 is one of the dominant serovars isolated from AIDS patients, but the biosynthesis of serovar 8-specific GPL remains unknown. To clarify this, we compared gene clusters involved in the biosynthesis of several serovar-specific GPLs and identified the genomic region predicted to be responsible for GPL biosynthesis in a serovar 8 strain. Sequencing of this region revealed the presence of four open reading frames, three unnamed genes and *gtfTB*, the function of which has not been elucidated. The simultaneous expression of *gtfTB* and two downstream genes in a recombinant *Mycobacterium smegmatis* strain genetically modified to produce serovar 1-specific GPL resulted in the appearance of 4,6-*O*-(1-carboxyethylidene)-3-*O*-methyl-glucose, which is unique to serovar 8-specific GPL, suggesting that these three genes participate in its biosynthesis. Furthermore, functional analyses of *gtfTB* indicated that it encodes a glucosyltransferase that transfers a glucose residue via 1→3 linkage to a rhamnose residue of serovar 1-specific GPL, which is critical to the formation of the oligosaccharide portion of serovar 8-specific GPL. Our findings might provide a clue to understanding the biosynthetic regulation that modulates the biological functions of GPLs in MAC.**

Mycobacteria are pathogens that cause diseases such as tuberculosis and leprosy. In addition, nontuberculous mycobacteria, which are widely distributed in the natural environment, cause opportunistic pulmonary infections resembling tuberculosis. These mycobacteria are distinguished by a multilayered cell envelope consisting of peptidoglycan, mycolyl arabinogalactan, and surface glycolipids (9, 13). The surface glycolipids are abundant and structurally different, and they may act as a barrier to immune responses (9, 13). Glycopeptidolipids (GPLs) are major glycolipid components present on the surface of several species of nontuberculous mycobacteria (40). All of these GPLs have a conserved core structure that is composed of a fatty acyl tetrapeptide glycosylated with 6-deoxytalose (6-d-Tal) and *O*-methyl-rhamnose (O-Me-Rha) and are termed non-serovar-specific GPLs (nsGPLs) (2, 4, 14). On the other hand, the GPLs of *Mycobacterium avium* complex (MAC), nontuberculous mycobacteria consisting principally of two species, *M. avium* and *M. intracellulare*, have various haptenic oligosaccharides linked to the 6-d-Tal residue of nsGPLs, resulting in serovar-specific GPLs (ssGPLs) (2, 4, 40). The oligosaccharide portions of ssGPLs define MAC serovars that are classified into 28 types. The serovar 1-specific GPL, with Rha linked to the 6-d-Tal residue, is the basic oligosaccharide unit of all ssGPLs (11). The Rha residue of serovar 1-specific GPL is further extended by various glycosylation steps, such as rhamnosylation, fucosylation, and glucosylation (11). These glycosylation steps generate structural diversity in GPLs of MAC (11). However, because of their complexity, most of the biosynthetic pathways for ssGPLs have not been fully determined. We recently showed that the biosynthesis of nsGPLs was regulated by a combination of glycosyltransferases (31). Therefore, each glycosyltransferase might mediate a specific step in the biosynthesis of ssGPLs.

In terms of biological activity, it has been reported that the properties of ssGPLs are notably different from each other and that some of the properties play a role in affecting host responses to MAC infections (3, 5, 21, 27, 37, 38). Moreover, epidemiological studies have shown that serovars 1, 4, and 8 are distributed predominantly in North America and are also frequently isolated from AIDS patients (24, 39, 41). However, in contrast to other ssGPLs, the serovar 8-specific GPL is reported to be able to induce altered immune responses (3, 21). The biosynthetic pathway for serovar 8-specific GPL, particularly its oligosaccharide portion that includes a unique 4,6-*O*-(1-carboxyethylidene)-3-*O*-methyl-glucose (Glc) residue (7, 8) that may determine the specificity of serovar 8, remains unknown (Table 1). In this study, we investigated the genomic region assumed to be associated with the biosynthesis of GPL in MAC serovar 8 strain and identified the genes involved in

* Corresponding author. Mailing address: Department of Microbiology, Leprosy Research Center, National Institute of Infectious Diseases, 4-2-1 Aobacho, Higashimurayama, Tokyo 189-0002, Japan. Phone: 81-42-391-8211. Fax: 81-42-394-9092. E-mail: yujim@nih.go.jp.

▽ Published ahead of print on 10 October 2008.

TABLE 1. Oligosaccharide structures of serovar 1- and 8-specific GPLs

Serovar	Oligosaccharide	Reference(s)
1	α-L-Rha-(1→2)-L-6-d-Tal	17
8	4,6-*O*-(1-carboxyethylidene)-3-*O*-methyl-β-D-Glc-(1→3)-α-L-Rha-(1→2)-L-6-d-Tal	7, 8

the glycosylation pathway leading to the formation of serovar 8-specific GPL.

MATERIALS AND METHODS

Bacterial strains, culture conditions, and DNA manipulation. Table 2 shows the bacterial strains and vectors used in this study. MAC strains were grown in Middlebrook 7H9 broth (Difco) with 0.05% Tween 80 supplemented with 10% Middlebrook ADC enrichment (BBL). Recombinant *M. smegmatis* strains used for GPL production were cultured in Luria-Bertani broth with 0.2% Tween 80. Isolation of DNA and transformation of *M. smegmatis* strains were performed as previously described (32). The genomic regions of MAC strains were amplified by a two-step PCR using TaKaRa *LA Taq* with GC buffer and the following program: denaturation at 98°C for 20 s and annealing-extension at 68°C for an appropriate time depending on the length of the targeted region. *Escherichia coli* strain DH5α was used for routine manipulation and propagation of plasmid DNA. When necessary, antibiotics were added as follows: kanamycin, 50 μg/ml for *E. coli* and 25 μg/ml for *M. smegmatis*; and hygromycin B, 150 μg/ml for *E. coli* and 75 μg/ml for *M. smegmatis*. Oligonucleotide primers used in this study are listed in Table 3.

Construction of expression vectors. The *rtfA* gene was amplified from genomic DNA of *M. avium* strain JATA51-01 using primers RTFA-S and RTFA-A. The PCR products were digested with each restriction enzyme and cloned into the BamHI-PstI site of pMV261 to obtain pMV-rtfA. To use the site-specific integrating mycobacterial vector more conveniently, we constructed pYM301a containing an AflII site in pYM301. The region encompassing *gtfTB*, ORF3, and ORF4 was amplified from genomic DNA of MAC serovar 8 strain ATCC 35771 using primers GTFTB-S and ORF4-A. In addition, *gtfTB* was amplified using primers GTFTB-S and GTFTB-A. The PCR products were digested with each restriction enzyme and cloned into the PstI-EcoRI site of pYM301a to obtain pYM-gtfTB-orf3-orf4 and pYM-gtfTB (Table 2).

Isolation and purification of GPLs. Harvested bacterial cells were allowed to stand in $CHCl_3$-CH_3OH (2:1, vol/vol) for several hours at room temperature. After water was added, total-lipid extracts were obtained from the organic phase and evaporated to dryness. Total-lipid extracts were subjected to mild alkaline hydrolysis as previously described (32, 33) to obtain crude GPL extracts. For analytical thin-layer chromatography (TLC), crude GPLs obtained from the same wet weight of harvested bacterial cells were spotted on Silica Gel 60 plates (Merck) using $CHCl_3$-CH_3OH-H_2O (30:8:1, vol/vol/vol) as the solvent and were visualized by spraying the plates with 10% H_2SO_4 and charring. Purified GPLs were prepared from crude GPLs by preparative TLC on the same plates, and each GPL was extracted from the corresponding band. Perdeuteriomethylation was carried out as previously described (6, 12, 17).

TABLE 3. Oligonucleotide primers used in this study

Primer	Sequence[a]	Restriction site
RTFA-S	5′-CGGGATCCCATGAAATTTGCTGTGGCAAG-3′	BamHI
RTFA-A	5′-AACTGCAGCTCAGCGACTTCGCTGCGCTTC-3′	PstI
GTFTB-S	5′-AACTGCAGAAATGACCGCCACAACCAGGGC-3′	PstI
GTFTB-A	5′-GGAATTCTCAGGCGCTCAGTGGCTCGTC-3′	EcoRI
ORF4-A	5′-GGAATTCCTAGGGCGCCAATTCGATGAG-3′	EcoRI
GTFB-U4	5′-GGAATTCGGTCGACTCGACGAAGCCGAC-3′	EcoRI
DRRC-A	5′-GGAATTCTGCAGGCGGGGCGACTCCTGCT-3′	EcoRI

[a] Underlining indicates restriction sites.

GC-MS and MALDI-TOF MS analysis. Crude and purified GPLs were hydrolyzed in 2 M trifluoroacetic acid (2 h, 120°C), and the released sugars were reduced with $NaBD_4$ and then acetylated with pyridine-acetic anhydride (1:1, vol/vol) at room temperature overnight. The resulting alditol acetates were separated and analyzed by gas chromatography-mass spectrometry (GC-MS) with a TRACE DSQ (Thermo Electron) equipped with an SP-2380 column (Supelco) using helium gas. The following program was used: temperature increased from 52 to 172°C at a rate of 40°C/min and then increased from 172 to 250°C at a rate of 3°C/min. To determine the total mass of the purified GPLs, matrix-assisted laser desorption ionization—time of flight (MALDI-TOF) mass spectra (in the positive mode) were obtained with a QSTAR XL (Applied Biosystems) using a pulse laser with emission at 337 nm. Samples mixed with 2,5-dihydroxybenzoic acid as the matrix were analyzed in the reflectron mode with an accelerating voltage of 20 kV and with operation in positive ion mode.

Nucleotide sequence accession number. The 4.6-kb genomic region amplified from MAC serovar 8 strain ATCC 35771 using primers GTFB-U4 and DRRC-A has been deposited in the DDBJ nucleotide sequence database under accession number AB437139.

RESULTS

Isolation and sequencing of the 4.6-kb genomic region responsible for GPL biosynthesis in MAC serovar 8. Lacking information on the genes responsible for biosynthesis of serovar 8-specific GPL, we compared and analyzed the genomic regions likely to be responsible for GPL biosynthesis in several

TABLE 2. Bacterial strains and vectors used in this study

Strain or vector	Characteristics	Source or reference
Bacteria		
E. coli DH5α	Cloning host	TaKaRa
M. smegmatis mc^{2}155	Expression host	35
M. intracellulare ATCC 35771	MAC serovar 8 strain	29
M. avium JATA51-01	Source of *rtfA*	17
Vectors		
pYM301	Source of pYM301a	30
pYM301a	Site-specific integrating mycobacterial vector carrying an *hsp60* promoter cassette and AflII site	This study
pMV261	*E. coli-Mycobacterium* shuttle vector carrying an *hsp60* promoter cassette	36
pMV-rtfA	pMV261 with *rtfA*	This study
pYM-gtfTB	pYM301a with *gtfTB*	This study
pYM-gtfTB-orf3-orf4	pYM301a with *gtfTB*, ORF3, and ORF4	This study

FIG. 1. Organization of the 4.6-kb genomic region isolated from MAC serovar 8 strain. Filled triangles indicate the primers used for PCR amplification.

MAC serovars (16, 28). Most of these regions have high homology to each other, while the segment between the *gtfB* and *drrC* genes was found to vary in the strains. Therefore, we assumed that this segment contains genes involved in the formation of the unique Glc residue in serovar 8-specific GPL. To clone the *gtfB-drrC* region by using PCR, we designed various primers containing sequences derived from other MAC strains. By examining combinations of several pairs of primers, a 4.6-kb fragment was amplified from genomic DNA of a MAC serovar 8 strain when primers GTFB-U4 and DRRC-A were used (Fig. 1). Sequencing of this 4.6-kb fragment revealed four complete open reading frames (Fig. 1). The deduced amino acid sequences encoded by ORF1, ORF2, ORF3, and ORF4 were found to be identical to the amino acid sequences of four functionally undefined proteins from *M. avium* strain 104, MAV_3253, MAV_3255, MAV_3256, and MAV_3257, respectively (GenBank accession no. NC_008595.1). *M. avium* strain A5 also possessed a genomic region harboring ORF2, ORF3, and ORF4 (GenBank accession no. AY130970.1). These four open reading frames are predicted to encode the following proteins: ORF1, a putative glycosyltransferase similar to GtfD, which has been identified as a fucosyltransferase involved in the biosynthesis of serovar 2-specific GPL (73% identity) (30); ORF2, a putative glycosyltransferase, designated GtfTB, showing high homology to Rv1516c of *M. tuberculosis* (61% identity) (28); ORF3, a putative polysaccharide pyruvyltransferase similar to MSMEG_4736 and MSMEG_4737 of *M. smegmatis* (61 and 58% identity, respectively) (GenBank accession no. NC_008596.1); and ORF4, a putative *O*-methyltransferase similar to MSMEG_4739 of *M. smegmatis* (55% identity) (GenBank accession no. NC_008596.1).

Identification of the genes required for synthesis of the sugar residue unique to serovar 8-specific GPL. Based on the deduced functions of the genes in the 4.6-kb fragment, we focused on *gtfTB* (ORF2), ORF3, and ORF4 and characterized them by performing expression analyses. Because the serovar 8-specific GPL has a structure in which the Rha residue of serovar 1-specific GPL is further glycosylated (Table 1), it was necessary to prepare a strain producing serovar 1-specific GPL that could be the substrate for the enzymes participating in the biosynthesis of serovar 8-specific GPL. For this, as previously demonstrated, we created a recombinant *M. smegmatis* strain, designated MS-S1, by introducing the plasmid vector pMV-rtfA having the *M. avium rtfA* gene, which converts nsGPLs to serovar 1-specific GPL (30). We then introduced the integrative expression vector pYM-gtfTB possessing *gtfTB* into MS-S1 and assessed GPL profiles by performing a TLC analysis (Fig. 2). By comparison with the profile of MS-S1/pYM301a (vector control) (Fig. 2, lane A), two new spots, designated spots GPL-SG-U and -D, were observed in MS-S1/pYM-gtfTB (Fig. 2, lane B), indicating that serovar 1-specific

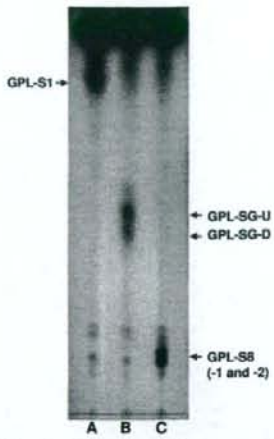

FIG. 2. TLC of crude GPL extracts from recombinant *M. smegmatis* strains MS-S1/pYM301a (A), MS-S1/pYM-gtfTB (B), and MS-S1/pYM-gtfTB-orf3-orf4 (C). GPL extracts were prepared from the total-lipid fraction, and this was followed by mild alkaline hydrolysis. Samples were spotted and developed using $CHCl_3$-CH_3OH-H_2O (30:8:1, vol/vol/vol).

GPL was converted to structurally different compounds by expression of *gtfTB*. Moreover, when the expression vector pYM-gtfTB-orf3-orf4 containing *gtfTB*, ORF3, and ORF4 was introduced into MS-S1, another new spot, designated GPL-S8, appeared (Fig. 2, lane C), implying that the structure of GPL-SG-U and -D was further modified by the products of ORF3 and ORF4. To confirm that these compounds contain the sugar residues associated with serovar 8-specific GPL, we performed a GC-MS analysis of the monosaccharides released from crude GPL extracts of each recombinant strain and the MAC serovar 8 strain (Fig. 3). The results showed that there was an excess of Glc, together with Rha, 6-d-Tal, 3,4-di-*O*-methyl-Rha, and 2,3,4-tri-*O*-methyl-Rha, in the profile of MS-S1/pYM-gtfTB compared with other profiles, as well as minor Glc peaks presumably derived from traces of trehalose-containing glycolipids (Fig. 3B). This indicates that the *gtfTB* gene mediates the transfer of a Glc residue to serovar 1-specific GPL. In contrast, the profile of MS-S1/pYM-gtfTB-orf3-orf4 revealed the presence of 4,6-*O*-(1-carboxyethylidene)-3-*O*-methyl-Glc, which was also detected in the MAC serovar 8 strain (Fig. 3C and D), demonstrating that the three genes are associated with the formation of the unique sugar residue of serovar 8-specific GPL.

Functional characterization of *gtfTB*. Expression analysis showed that serovar 1-specific GPL was converted to new compounds containing Glc when the *gtfTB* gene was expressed (Fig. 2, lane B, and Fig. 3B). Although these results suggested that the product of *gtfTB* participates in the formation of a Glc residue, it is not clear whether *gtfTB* encodes the glycosyltransferase that transfers Glc via 1→3 linkage to the Rha residue of serovar 1-specific GPL, whose linkage was previously detected in serovar 8-specific GPL (7, 8). To elucidate the function of *gtfTB*, we determined the linkage of sugar moieties of GPL-SG-U and -D, which were produced by recombinant strain

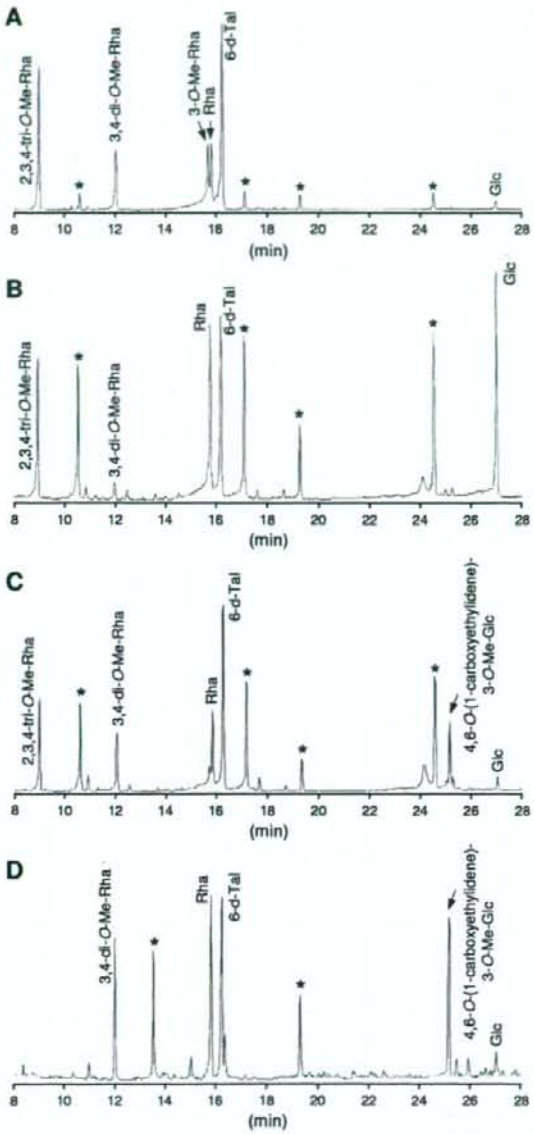

FIG. 3. GC-MS of alditol acetate derivatives from crude GPL extracts of recombinant strains *M. smegmatis* MS-S1/pYM301a (A), MS-S1/pYM-gtfTB (B), and MS-S1/pYM-gtfTB-orf3-orf4 (C) and a MAC serovar 8 strain (D). GPL extracts were prepared from the total-lipid fraction, and this was followed by mild alkaline hydrolysis. Asterisks indicate noncarbohydrates. Me, methyl.

MS-S1/pYM-gtfTB (Fig. 2, lane B). After extraction of the products from the corresponding bands on the TLC plate, purified GPL-SG-U and -D were subjected to perdeuteriomethylation followed by GC-MS. The differences in the TLC profiles of GPL-SG-U and -D might have been due to the presence or absence of fatty acid methylation, which is often observed in *M. smegmatis* GPLs (23, 31), whereas the GC-MS profiles and fragmentation ions for GPL-SG-U and -D were identical, demonstrating that GPL-SG-U and -D had the same sugar moieties and linkages. Therefore, the profiles of GPL-SG-U shown here are representative of GPL-SG-U and -D. The GC-MS profile of GPL-SG-U contained four peaks corresponding to 6-d-Tal, Rha, Glc, and 2,3,4-tri-*O*-methyl-Rha (data not shown). The characteristic spectra for Glc, Rha, and 6-d-Tal are shown in Fig. 4. The spectrum of Glc had fragment ions at *m/z* 121, 167, and 168, which represent the presence of deuteriomethyl groups at positions C-2, C-3, and C-4 (Fig. 4A). In contrast, fragment ions at *m/z* 121, 134, 193, and 240 were detected for Rha, indicating that a deuteriomethyl group was introduced at positions C-2 and C-4 of Rha, in which position C-3 was acetylated (Fig. 4B). In addition, detection of fragment ions at *m/z* 134, 181, and 193 (Fig. 4C) revealed that there was deuteriomethylation at positions C-3 and C-4 in 6-d-Tal. These results demonstrated that position C-1 of Glc is linked to position C-3 of Rha but not to position C-2 of 6-d-Tal, because it has been determined previously that position C-1 of Rha is linked to position C-2 of 6-d-Tal in the oligosaccharide of serovar 1-specific GPL (17). Accordingly, the oligosaccharide structures of GPL-SG-U and -D were determined to have Glc-(1→3)-Rha-(1→2)-6-d-Tal at D-*allo*-Thr, demonstrating that *gtfTB* encodes the glucosyltransferase that transfers a Glc residue via 1→3 linkage to the Rha residue of serovar 1-specific GPL.

Structural assignment of GPL-S8 synthesized by expression of *gtfTB*, ORF3, and ORF4. GC-MS of the crude GPL extract from MS-S1/pYM-gtfTB-orf3-orf4 revealed the presence of 4,6-*O*-(1-carboxyethylidene)-3-*O*-methyl-Glc (Fig. 3C). To confirm that this structural component was derived from GPL-S8, we performed GC-MS and MALDI-TOF MS analyses of purified GPL-S8. The results showed that GPL-S8 contained a 4,6-*O*-(1-carboxyethylidene)-3-*O*-methyl-Glc residue and two main pseudomolecular ions (*m/z* 1,565.9 and 1,579.8 $[M + Na]^+$) (data not shown). Consequently, as shown in Fig. 5, these results were consistent with the proposed structure for GPL-S8-1 and -2 containing 4,6-*O*-(1-carboxyethylidene)-3-*O*-methyl-Glc, with differences in pseudomolecular ions due to fatty acid methylation.

DISCUSSION

Structural diversity of the ssGPLs, notably in their sugar residues, defines 28 serovars of MAC. Although these ssGPLs are known to contribute to the virulence of MAC, the mechanisms of their biosynthetic regulation are largely unknown. In this study, we clarified the biosynthetic pathway for serovar 8-specific GPL, specifically the glycosylation step in which a Glc residue is transferred to the Rha residue of serovar 1-specific GPL.

To isolate the genomic region associated with the biosynthesis of serovar 8-specific GPL, we compared the GPL biosynthetic gene clusters in several MAC strains and found significant differences in the *gtfB-drrC* region. The segment flanking the 3′ end of the *gtfB-drrC* region includes several genes responsible for the serovar 1-specific GPL whose structure is found in all ssGPLs. On the other hand, it is experimentally

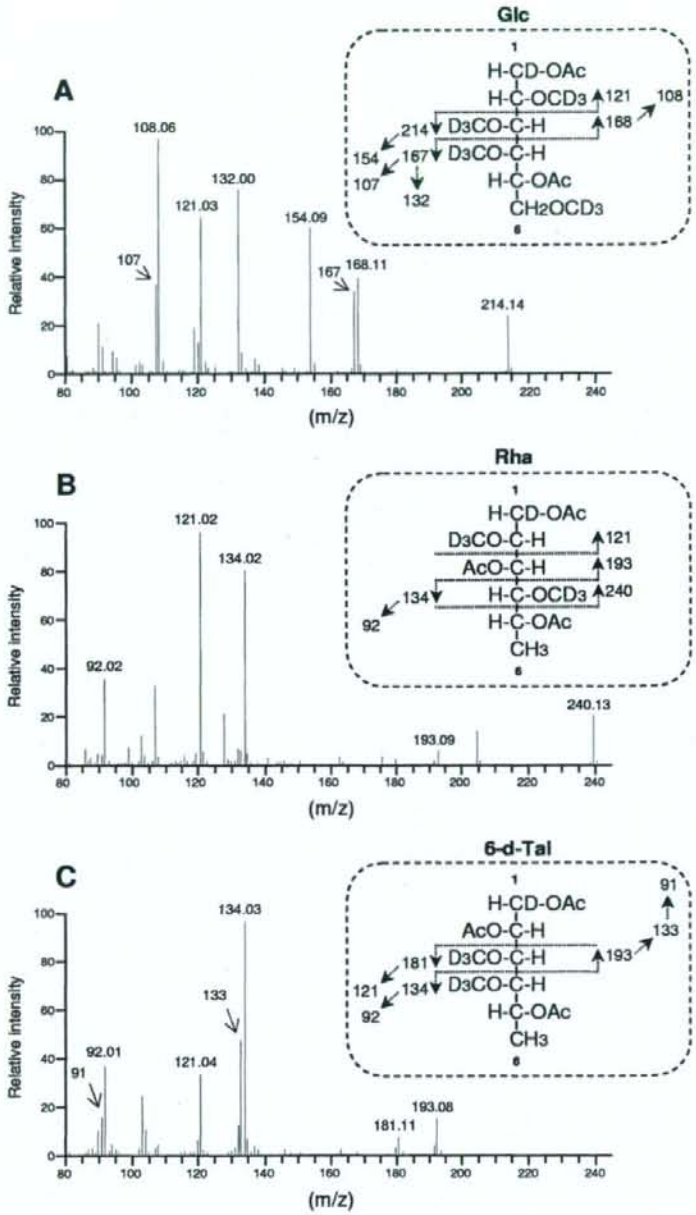

FIG. 4. GC-MS spectra and fragment ion assignments for Glc (A), Rha (B), and 6-d-Tal (C), which were derived from alditol acetates of sugars released from deuteriomethylated GPL-SG-U. Ac, acetate; D, deuterium.

clarified that the *gtfB-drrC* regions of serovar 2-, 7-, and 16-specific GPL-producing strains contain the genes involved in the formation of the specific sugar residues that are transferred to the Rha residue of serovar 1-specific GPL (18, 19, 30). Thus, this region could play an important role in generating the structural diversity of ssGPLs. As shown in this study, the specific functions for formation of sugar moieties of serovar 8-specific GPL were due to the genes present in the *gtfB-drrC*

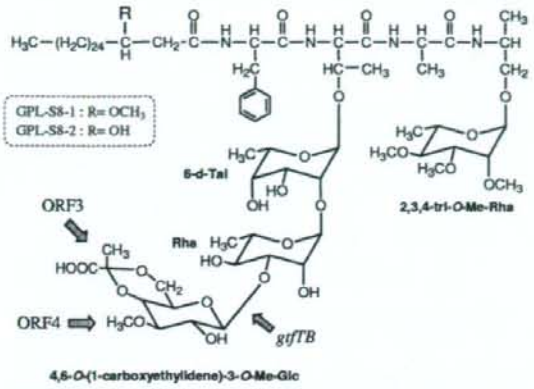

FIG. 5. Proposed structure and biosynthetic genes of GPL-S8 (serovar 8-specific GPL). Me, methyl.

region, suggesting that focusing on this region might provide clues for elucidating the characteristics of other ssGPLs whose biosynthesis is still not known.

It has been reported previously that the *gtfTB* gene in *M. avium* strains 104 and A5 was not likely to be associated with GPL biosynthesis because its ancestral homologue, Rv1516c (61% identity with the GtfTB gene), was the gene of *M. tuberculosis*, which produces no GPLs (28). Thus, it was interesting that *gtfTB* encodes a glycosyltransferase that does participate in GPL biosynthesis in which a Glc residue is transferred to serovar 1-specific GPL, yielding the serovar 8-specific GPL. *M. avium* strains 104 and A5 synthesize serovar 1-specific GPL as a final product and intermediate, respectively, while it has been recognized that neither of these strains produces serovar 8-specific GPL in spite of the presence of *gtfTB* in the GPL biosynthetic gene cluster (28). These observations raised the possibility that the transcription of *gtfTB* is inefficient in both strains due to the upstream sequences. Actually, in *M. avium* strain 104, a transposase sequence was observed upstream of *gtfTB*, indicating that this strain might be deficient in glucosylation, and consequently a serovar 1-specific GPL-producing strain is obtained (28). On the other hand, it has been shown that the biosynthetic gene cluster for serovar 7-specific GPL in *M. intracellulare* strain ATCC 35847 contains a putative glycosyltransferase gene which encodes amino acid sequences that are similar to the amino acid sequences encoded by *gtfTB* (59% identity) (18). Structural analysis of sugar moieties in serovar 7-specific GPL indicated that this GtfTB homologue may serve as a glycosyltransferase during formation of the terminal amidohexose residue that structurally resembles Glc (18).

The deduced amino acid sequences encoded by ORF3 and ORF4 showed that these genes putatively encode polysaccharide pyruvyltransferase and *O*-methyltransferase, respectively. Expression of ORF3 and ORF4 together with *gtfTB* led to structural alterations in which Glc was modified with both 4,6-*O*-(1-carboxyethylidene) and 3-*O*-methyl groups. Based on these observations, it is strongly suggested that ORF3 is associated with the formation of the 4,6-*O*-(1-carboxyethylidene) group that is synonymous with the cyclic pyruvate ketal and that ORF4 is associated with the 3-*O*-methylation of the Glc residue (Fig. 5). In mycobacteria, homologues of ORF3 and ORF4 were found only in *M. smegmatis*, as MSMEG_4736 (for ORF3), MSMEG_4737 (for ORF3), and MSMEG_4739 (for ORF4). *M. smegmatis* also produces glycolipids containing 4,6-*O*-(1-carboxyethylidene)-3-*O*-methyl-Glc as a sugar moiety (25, 34), which suggests that both homologues participate in the synthesis of these glycolipids. Sugar residues with a 4,6-*O*-(1-carboxyethylidene) group substitution have been found in carbohydrates such as extracellular polysaccharide and N-linked glycan, which are produced by some bacteria and yeasts (1, 15, 20, 22, 26). It has been shown that an increase in 4,6-*O*-(1-carboxyethylidene)-containing sugar residues leads to enhanced viscosity of extracellular polysaccharide from *Xanthomonas* sp., which alters the cell surface properties related to cellular attachment and protection from environmental stress (10). Accordingly, in terms of the properties of serovar 8-specific GPL, the presence of the 4,6-*O*-(1-carboxyethylidene) group might influence the pathogenicity of MAC serovar 8.

With regard to the antibody reactivity, it is unclear whether serovar 8-specific antibodies react with GPL-S8 because there are minor structural differences in the methylated positions of fatty acids and the terminal Rha residue linked to the tetrapeptide between GPL-S8 and serovar 8-specific GPL of MAC. Evaluation of the antibody response to GPL-S8 using serovar 8-specific antibodies would facilitate understanding the immunoreactivity mediated by ssGPLs.

In this study, we proved that *gtfTB* and adjacent genes in the GPL biosynthetic gene cluster in MAC serovar 8 strain are responsible for the formation of a unique glucose residue in serovar 8-specific GPL (Fig. 5). In particular, *gtfTB* encodes the glucosyltransferase that plays a critical role in the pathway leading from serovar 1-specific GPL to serovar 8-specific GPL. Through further study, including generation of *gtfTB* knockout mutants of MAC serovar 8 strains, results relevant to the biosynthesis of serovar 8-specific GPL might help clarify the biological function of ssGPLs and their role in the host-pathogen relationships of MAC.

ACKNOWLEDGMENTS

This study was supported in part by a Grant-in-Aid for Young Scientists (B) from the Ministry of Education, Culture, Science and Technology of Japan and Research on Emerging and Re-Emerging Infectious Diseases from the Ministry of Health, Labor and Welfare of Japan.

REFERENCES

1. **Aman, P., M. McNeil, L.-E. Franzen, A. G. Darvill, and P. Albersheim.** 1981. Structural elucidation, using HPLC-MS and GLC-MS, of the acidic exopolysaccharide secreted by *Rhizobium meliloti* strain Rm1021. Carbohydr. Res. **95**:263–282.
2. **Aspinall, G. O., D. Chatterjee, and P. J. Brennan.** 1995. The variable surface glycolipids of mycobacteria: structures, synthesis of epitopes, and biological properties. Adv. Carbohydr. Chem. Biochem. **51**:169–242.
3. **Barrow, W. W., T. L. Davis, E. L. Wright, V. Labrousse, M. Bachelet, and N. Rastogi.** 1995. Immunomodulatory spectrum of lipids associated with *Mycobacterium avium* serovar 8. Infect. Immun. **63**:126–133.
4. **Belisle, J. T., K. Klaczkiewicz, P. J. Brennan, W. R. Jacobs, Jr., and J. M. Inamine.** 1993. Rough morphological variants of *Mycobacterium avium*. Characterization of genomic deletions resulting in the loss of glycopeptidolipid expression. J. Biol. Chem. **268**:10517–10523.
5. **Bhatnagar, S., and J. S. Schorey.** 2007. Exosomes released from infected macrophages contain *Mycobacterium avium* glycopeptidolipids and are proinflammatory. J. Biol. Chem. **282**:25779–25789.
6. **Bjorndal, H., C. G. Hellerqvist, B. Lindberg, and S. Svensson.** 1970. Gas-liquid chromatography and mass spectrometry in methylation analysis of polysaccharides. Angew. Chem. Int. Ed. Engl. **9**:610–619.

7. **Brennan, P. J., G. O. Aspinall, and J. E. Shin.** 1981. Structure of the specific oligosaccharides from the glycopeptidolipid antigens of serovars in the *Mycobacterium avium-Mycobacterium intracellulare-Mycobacterium scrofulaceum* complex. J. Biol. Chem. **256:**6817–6822.
8. **Brennan, P. J., H. Mayer, G. O. Aspinall, and J. E. Nam Shin.** 1981. Structures of the glycopeptidolipid antigens from serovars in the *Mycobacterium avium/Mycobacterium intracellulare/Mycobacterium scrofulaceum* serocomplex. Eur. J. Biochem. **115:**7–15.
9. **Brennan, P. J., and H. Nikaido.** 1995. The envelope of mycobacteria. Annu. Rev. Biochem. **64:**29–63.
10. **Casas, J. A., V. E. Santos, and F. Garcia-Ochoa.** 2000. Xanthan gum production under several operational conditions: molecular structure and rheological properties. Enzyme Microb. Technol. **26:**282–291.
11. **Chatterjee, D., and K. H. Khoo.** 2001. The surface glycopeptidolipids of mycobacteria: structures and biological properties. Cell. Mol. Life Sci. **58:** 2018–2042.
12. **Ciucanu, I., and F. Kerek.** 1984. A simple and rapid method for the permethylation of carbohydrates. Carbohydr. Res. **131:**209–217.
13. **Daffe, M., and P. Draper.** 1998. The envelope layers of mycobacteria with reference to their pathogenicity. Adv. Microb. Physiol. **39:**131–203.
14. **Daffe, M., M. A. Laneelle, and G. Puzo.** 1983. Structural elucidation by field desorption and electron-impact mass spectrometry of the C-mycosides isolated from *Mycobacterium smegmatis*. Biochim. Biophys. Acta **751:**439–443.
15. **D'Haeze, W., J. Glushka, R. De Rycke, M. Holsters, and R. W. Carlson.** 2004. Structural characterization of extracellular polysaccharides of *Azorhizobium caulinodans* and importance for nodule initiation on *Sesbania rostrata*. Mol. Microbiol. **52:**485–500.
16. **Eckstein, T. M., J. T. Belisle, and J. M. Inamine.** 2003. Proposed pathway for the biosynthesis of serovar-specific glycopeptidolipids in *Mycobacterium avium* serovar 2. Microbiology **149:**2797–2807.
17. **Eckstein, T. M., F. S. Silbaq, D. Chatterjee, N. J. Kelly, P. J. Brennan, and J. T. Belisle.** 1998. Identification and recombinant expression of a *Mycobacterium avium* rhamnosyltransferase gene (*rtfA*) involved in glycopeptidolipid biosynthesis. J. Bacteriol. **180:**5567–5573.
18. **Fujiwara, N., N. Nakata, S. Maeda, T. Naka, M. Doe, I. Yano, and K. Kobayashi.** 2007. Structural characterization of a specific glycopeptidolipid containing a novel *N*-*acyl*-deoxy sugar from *Mycobacterium intracellulare* serotype 7 and genetic analysis of its glycosylation pathway. J. Bacteriol. **189:**1099–1108.
19. **Fujiwara, N., N. Nakata, T. Naka, I. Yano, M. Doe, D. Chatterjee, M. McNeil, P. J. Brennan, K. Kobayashi, M. Makino, S. Matsumoto, H. Ogura, and S. Maeda.** 2008. Structural analysis and biosynthesis gene cluster of an antigenic glycopeptidolipid from *Mycobacterium intracellulare*. J. Bacteriol. **190:**3613–3621.
20. **Gemmill, T. R., and R. B. Trimble.** 1996. *Schizosaccharomyces pombe* produces novel pyruvate-containing N-linked oligosaccharides. J. Biol. Chem. **271:**25945–25949.
21. **Horgen, L., E. L. Barrow, W. W. Barrow, and N. Rastogi.** 2000. Exposure of human peripheral blood mononuclear cells to total lipids and serovar-specific glycopeptidolipids from *Mycobacterium avium* serovars 4 and 8 results in inhibition of TH1-type responses. Microb. Pathog. **29:**9–16.
22. **Jansson, P. E., L. Kenne, and B. Lindberg.** 1975. Structure of extracellular polysaccharide from *Xanthomonas campestris*. Carbohydr. Res. **45:**275–282.
23. **Jeevarajah, D., J. H. Patterson, M. J. McConville, and H. Billman-Jacobe.** 2002. Modification of glycopeptidolipids by an *O*-methyltransferase of *Mycobacterium smegmatis*. Microbiology **148:**3079–3087.
24. **Julander, I., S. Hoffner, B. Petrini, and L. Ostlund.** 1996. Multiple serovars of *Mycobacterium avium* complex in patients with AIDS. APMIS **104:**318–320.
25. **Kamisango, K., S. Saadat, A. Dell, and C. E. Ballou.** 1985. Pyruvylated glycolipids from *Mycobacterium smegmatis*. Nature and location of the lipid components. J. Biol. Chem. **260:**4117–4121.
26. **Kojima, N., S. Kaya, Y. Araki, and E. Ito.** 1988. Pyruvic-acid-containing polysaccharide in the cell wall of *Bacillus polymyxa* AHU 1385. Eur. J. Biochem. **174:**255–260.
27. **Krzywinska, E., S. Bhatnagar, L. Sweet, D. Chatterjee, and J. S. Schorey.** 2005. *Mycobacterium avium* 104 deleted of the methyltransferase D gene by allelic replacement lacks serotype-specific glycopeptidolipids and shows attenuated virulence in mice. Mol. Microbiol. **56:**1262–1273.
28. **Krzywinska, E., and J. S. Schorey.** 2003. Characterization of genetic differences between *Mycobacterium avium* subsp. *avium* strains of diverse virulence with a focus on the glycopeptidolipid biosynthesis cluster. Vet. Microbiol. **91:**249–264.
29. **Li, Z., G. H. Bai, C. F. von Reyn, P. Marino, M. J. Brennan, N. Gine, and S. L. Morris.** 1996. Rapid detection of *Mycobacterium avium* in stool samples from AIDS patients by immunomagnetic PCR. J. Clin. Microbiol. **34:**1903–1907.
30. **Miyamoto, Y., T. Mukai, Y. Maeda, N. Nakata, M. Kai, T. Naka, I. Yano, and M. Makino.** 2007. Characterization of the fucosylation pathway in the biosynthesis of glycopeptidolipids from *Mycobacterium avium* complex. J. Bacteriol. **189:**5515–5522.
31. **Miyamoto, Y., T. Mukai, N. Nakata, Y. Maeda, M. Kai, T. Naka, I. Yano, and M. Makino.** 2006. Identification and characterization of the genes involved in glycosylation pathways of mycobacterial glycopeptidolipid biosynthesis. J. Bacteriol. **188:**86–95.
32. **Miyamoto, Y., T. Mukai, F. Takeshita, N. Nakata, Y. Maeda, M. Kai, and M. Makino.** 2004. Aggregation of mycobacteria caused by disruption of fibronectin-attachment protein-encoding gene. FEMS Microbiol. Lett. **236:**227–234.
33. **Patterson, J. H., M. J. McConville, R. E. Haites, R. L. Coppel, and H. Billman-Jacobe.** 2000. Identification of a methyltransferase from *Mycobacterium smegmatis* involved in glycopeptidolipid synthesis. J. Biol. Chem. **275:**24900–24906.
34. **Saadat, S., and C. E. Ballou.** 1983. Pyruvylated glycolipids from *Mycobacterium smegmatis*. Structures of two oligosaccharide components. J. Biol. Chem. **258:**1813–1818.
35. **Snapper, S. B., R. E. Melton, S. Mustafa, T. Kieser, and W. R. Jacobs, Jr.** 1990. Isolation and characterization of efficient plasmid transformation mutants of *Mycobacterium smegmatis*. Mol. Microbiol. **4:**1911–1919.
36. **Stover, C. K., V. F. de la Cruz, T. R. Fuerst, J. E. Burlein, L. A. Benson, L. T. Bennett, G. P. Bansal, J. F. Young, M. H. Lee, G. F. Hatfull, S. B. Snapper, R. G. Barletta, W. R. Jacobs, Jr., and B. R. Bloom.** 1991. New use of BCG for recombinant vaccines. Nature **351:**456–460.
37. **Sweet, L., and J. S. Schorey.** 2006. Glycopeptidolipids from *Mycobacterium avium* promote macrophage activation in a TLR2- and MyD88-dependent manner. J. Leukoc. Biol. **80:**415–423.
38. **Tassell, S. K., M. Pourshafie, E. L. Wright, M. G. Richmond, and W. W. Barrow.** 1992. Modified lymphocyte response to mitogens induced by the lipopeptide fragment derived from *Mycobacterium avium* serovar-specific glycopeptidolipids. Infect. Immun. **60:**706–711.
39. **Tsang, A. Y., J. C. Denner, P. J. Brennan, and J. K. McClatchy.** 1992. Clinical and epidemiological importance of typing of *Mycobacterium avium* complex isolates. J. Clin. Microbiol. **30:**479–484.
40. **Vergne, I., and M. Daffe.** 1998. Interaction of mycobacterial glycolipids with host cells. Front. Biosci. **3:**d865–876.
41. **Yakrus, M. A., and R. C. Good.** 1990. Geographic distribution, frequency, and specimen source of *Mycobacterium avium* complex serotypes isolated from patients with acquired immunodeficiency syndrome. J. Clin. Microbiol. **28:**926–929.

Tohoku J. Exp. Med., 2008, **216**, 363-370

Higher Susceptibility of Type 1 Diabetic Rats to *Mycobacterium tuberculosis* Infection

ISAMU SUGAWARA[1] and SATORU MIZUNO[1]

[1]Mycobacterial Reference Center, The Research Institute of Tuberculosis, Japan Anti-Tuberculosis Association, Tokyo, Japan

An association between diabetes mellitus and tuberculosis has been implicated for a long time. We have previously reported that Goto Kakizaki type 2 diabetic rats are highly susceptible to *Mycobacterium (M.) tuberculosis* infection. As a next step, we attempted to clarify whether type 1 diabetic rats are more susceptible to *M. tuberculosis* than non-diabetic wild-type (WT) rats. Here, we used the Komeda diabetes-prone (KDP) rat, as a model of type 1 diabetes mellitus. The infected KDP rats developed large granulomas without central necrosis in their lungs, liver or spleen. This was consistent with a significant increase in the number of colony-forming units (cfu) of *M. tuberculosis* in the lungs and spleen ($p < 0.01$). Insulin treatment resulted in significant reduction of tubercle bacilli in the infected KDP rats ($p < 0.01$). Pulmonary levels of interferon-γ, tumor necrosis factor-α and interleukin-1β mRNAs were higher in the infected diabetic rats than in WT rats. Alveolar macrophages from KDP rats were not fully activated by *M. tuberculosis* infection because the macrophages did not secrete nitric oxide (NO) that can kill *M. tuberculosis* ($p < 0.01$), but no significant difference in phagocytosis of tubercle bacilli by alveolar macrophages was observed between KDP and WT rats. Taken together, our findings indicate that type 1 diabetic rats are more susceptible to *M. tuberculosis* that WT rats.

——— type 1 diabetic rat; type 1 diabetes mellitus; tuberculosis; cytokine.

Tohoku J. Exp. Med., 2008, **216** (4), 363-370.

© 2008 Tohoku University Medical Press

Patients with diabetes mellitus (DM) seem to be at high risk of developing tuberculosis, and DM is one of the risk factors for tuberculosis. It has been implicated that there is a clinical link between diabetes mellitus and pulmonary tuberculosis (Garay 2004), and several studies have investigated this issue (Banyai 1931; Root 1934; Boucot et al. 1952; Kim et al. 1995). As patients with DM are increasing worldwide, it is important to examine why diabetic patients are susceptible to *M. tuberculosis* infection.

DM is broadly classified into two types: type 1 (insulin-dependent) and type 2 (insulin-independent) (Powers 2008). There are several animal models of DM including non-obese diabetic (NOD) mice and spontaneously diabetic Goto Kakizaki (GK) rats (Goto et al. 1976; Makino et al. 1976). When GK rats were used to examine the relationship between type 2 DM and tuberculosis, we found that the rats developed large granulomas and that their alveolar macrophages were not fully activated by *Mycobacterium (M.) tuberculosis* infection (Sugawara et al. 2004). This was consistent with the significantly increased

Received August 21, 2008; revision accepted for publication November 11, 2008.

Correspondence: Dr. Isamu Sugawara, Mycobacterial Reference Center, The Research Institute of Tuberculosis, 3-1-24 Matsuyama, Kiyose, Tokyo 204-0022, Japan.
e-mail: sugawara@jata.or.jp

number of colony-forming units of *M. tuberculosis* in the lung and spleen tissues.

We then examined the relationship between type 1 DM and experimental tuberculosis. As at the time there was no rat model of type 1 diabetes, NOD type 1 mice were utilized instead for this purpose. The results were variable and inconsistent. NOD mice developed large granulomas in one experiment, but not in another experiment. It has been reported previously that NOD mice are resistant to *M. avium* and that the infection prevents autoimmune disease (Bras and Aguas 1996). Moreover, protection of NOD mice from diabetes is a Th1-type response that is mediated by up-regulation of the Fas-FasL pathway and involves an increase in the cytotoxicity of T cells (Martins and Aguas 1999). Clearly, the pathogenesis of tuberculosis in NOD mice is a complex process and requires further clarification.

A rat model of type1 diabetes was eventually developed in 1998 in Japan, and was named the Komeda diabetes-prone (KDP) rat (Komeda et al. 1998; Yokoi et al. 2003). It is reported that Cb1b, a member of the Cbl/Sli family of ubiquitin-protein ligases, is a major susceptibility gene for rat type 1 diabetes mellitus (Yokoi et al. 2002). This research background led us to re-examine the pathophysiology of pulmonary tuberculosis in type 1 diabetic rats. Our results suggest that type 1 diabetic rats are more susceptible to *M. tuberculosis* infection than non-diabetic rats.

Materials and Methods

Animals

Six-week-old female type 1 diabetic rats and sex- and age-matched control Long-Evans Tokushima lean (LETL) rats were purchased from SLC Co. (Shizuoka, Japan) (Komeda et al. 1998). The diabetic rats are not obese and develop insulitis with lymphocyte infiltration over time, being responsive to rabbit insulin, which ameliorates the diabetes. Hyperlipidemia and hypercholesterolemia are not recognized in KDP rats. The blood glucose level in this model was measured with an Ascensia Brio blood glucose measurement apparatus (Bayer Medical Co., Tokyo, Japan) with a measurement range of 30-550 mg/dl. All rats were housed in a biosafety level 3 facility and given rat chow and water *ad libitum* after aerosol infection with *M. tuberculosis* Kurono strain. The degree of severity of type 1 DM in the diabetic rats was evaluated mainly by assessment of blood glucose levels. Blood glucose levels in the rats were between 200 and 550 mg/dl.

Experimental infections

The Kurono strain of *M. tuberculosis* (ATCC35812) was grown in Middlebrook 7H9 broth for two weeks, and then filtered with a sterile acrodisc syringe filter with a pore size of 5.0 μm. Aliquots of the bacterial filtrate were stored at −80°C until use. The diabetic and WT rats were infected via the airborne route by placing them in an exposure chamber in a Glas-Col aerosol generator (Glas-Col, Inc., Terre Haute, IN, USA) (Sugawara et al. 2004). The nebulizer compartment was filled with 5 ml of a suspension containing 3×10^6 colony-forming units (cfu) of Kurono tubercle bacilli so that approximately 200 bacteria would potentially be deposited in the lungs of each animal. Inhalation infection experiments were carried out twice.

For some experiments, the diabetic rats were treated with 100 μl rabbit insulin (10 ng/ml, Shibayagi Co., Takasaki, Gunma, Japan) twice daily from the day after aerosol infection. The blood glucose level of the insulin-treated KDP rats was less than 200 mg/dl. Permission to perform the experiments on the animals was granted by the Animal Experiment Committee at the Research Institute of Tuberculosis.

Colony-forming unit (cfu) assay

At 7 weeks after aerosol infection, the rats were anesthetized with pentobarbital sodium. The right lobe of each lung and part of the spleen tissue were weighed and used to evaluate the *in vivo* growth of mycobacteria. The lung and spleen tissues were homogenized with a mortar and pestle, and 1 ml of a sterile dilution of the homogenate was cultured on 1% Ogawa egg medium. Colonies were counted after four weeks of incubation at 37°C (Yamada et al. 2001).

In vitro effect of glucose on mycobacterial growth

Diabetes is characterized by hyperglycemia. In order to examine the *in vitro* effect of glucose on *M. tuberculosis* growth, 0.1%, 0.5% and 1% glucose (w/v) was added to *M. tuberculosis* Kurono strain in 7H9 medium and the mixture was cultured for one week. Thereafter, the 10-fold-diluted culture suspension was cultured on 1% Ogawa egg medium for four weeks and the colonies

were counted.

Histopathology

For light microscopy, the rats were sacrificed seven weeks after infection. Tissue sections were cut from paraffin blocks containing lung, liver or spleen tissue and stained with hematoxylin and eosin or by the Ziehl-Neelsen method for acid-fast bacilli (Sugawara et al. 2004).

Real-time PCR

Another portion of the remaining right lower lobes of the lungs was used for reverse transcriptase PCR (RT-PCR) analysis to examine the expression levels of several cytokine mRNAs in these samples during *M. tuberculosis* infection. These samples were snap-frozen in liquid nitrogen and stored at −85°C until use. RNA extraction was performed as described previously (Yamada et al. 2005). Briefly, the frozen tissues were homogenized in a microcentrifuge tube with an autoclaved disposable 1000-μL tip cooled by dipping in liquid nitrogen. Then the homogenates were treated with 1 mL of TRIzol reagent (Invitrogen Japan Co., Tokyo, Japan), as specified by the manufacturer. After RNA isolation, total RNA concentration was measured with a spectrophotometer, and the agarose gel electrophoresis pattern of the total RNA was examined. The total RNAs were reverse-transcribed into cDNA with Moloney murine leukemia virus reverse transcriptase (Invitrogen). ABI Taqman® Gene Expression Assay was used for relative quantitative measurement of the mRNA expression of interferon (IFN)-γ, tumor necrosis factor (TNF)-α, and interleukin (IL)-1β (Yamada et al. 2005). A TaqMan® Rodent GAPDH Control Reagents set was used for normalization for data analysis. Real-time RT-PCR was performed according to the instructions for the ABI PRISM 7900HT Sequence Detection System (Applied BioSystems Inc.). Data were analyzed by the $\Delta\Delta C_T$ method using the ABI PRISM Sequence Detection System software package (version 2.1; Applied BioSystems, California, USA) running on Windows 2000. The results obtained from diabetic and control rats were expressed as relative expression quantities of the targets in comparison with those of non-infected rats that were calibrated with the expression of an internal control gene glyaraldehyde-3-phosphate dehydrogenase (GAPDH) (Yamada et al. 2005; Yamada et al. 2007).

Alveolar macrophage nitric oxide (NO) assay

Alveolar macrophages (3×10^6/well) were plated in 96-well culture plates in RPMI 1640 (Sigma-Aldridge, St. Louis, MO, USA) supplemented with 10% heat-inactivated fetal calf serum and then stimulated with *M. tuberculosis* Kurono strain and cultured overnight. The supernatants were collected 16 hours after culture seeding, filtered, and their NO concentrations were determined by the Griess assay as described previously (Green et al. 1990; Sugawara et al. 2004).

Statistical analysis

All values were expressed as means±S.E. and compared using Student's t test. For all statistical analyses, the level of statistical significance was set at $p < 0.01$.

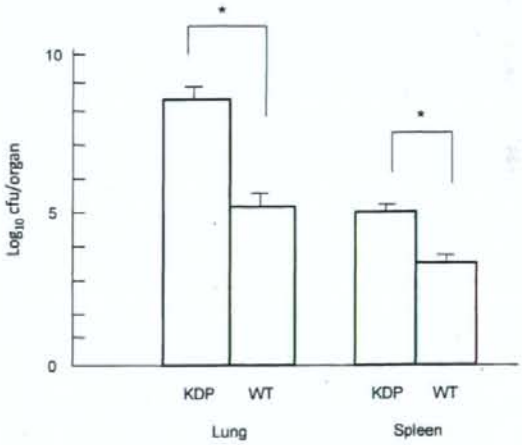

Fig. 1. Mycobacterial burden in the lung and spleen tissue of type 1 diabetic rats.
Colony-forming units (cfu) in lung and spleen tissues from type 1 diabetic (KDP) rats and wild-type rats exposed to 3×10^6 cfu of *M. tuberculosis* Kurono strain by aerosol infection. Seven weeks after infection, three rats from each group were sacrificed, and homogenates of the lungs and spleen were cultured. There is a significant difference in the lung and spleen cfu counts between KDP and WT rats ($p < 0.01$).
Error bars indicate standard deviation (SD) from the mean. *$p < 0.01$ vs. WT rats.

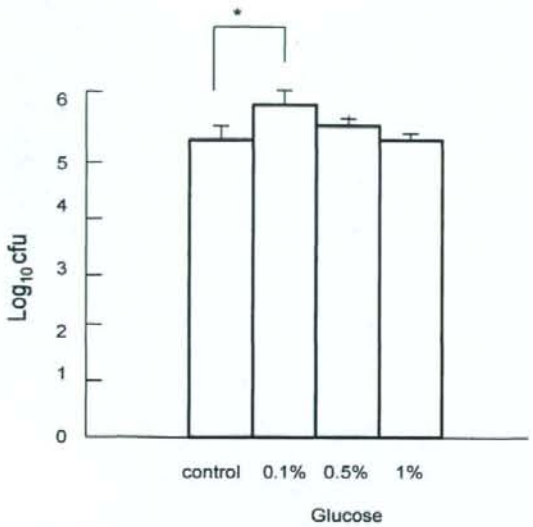

Fig. 2. *In vivo* effect of insulin treatment on tubercle bacilli in granulomas.
Type 1 diabetic (KDP) rats were treated with 100 μl rabbit insulin (10 ng/ml, Shibayagi Co., Takasaki, Gunma, Japan) twice daily from the day after aerosol infection. *$p < 0.01$ vs. WT rats.

Results

Mycobacterial burden in the lung and spleen tissue of KDP rats

When diabetic and WT LETL rats were infected via the airborne route with the Kurono strain of *M. tuberculosis* (3×10^6), all rats survived until the date of sacrifice (49 days after infection). As shown in Fig. 1, the number of mycobacterial colonies in the lung and spleen tissues increased, and there was a significant difference in the lung and spleen cfu counts between diabetic and WT rats ($p < 0.01$).

When insulin was administered to the diabetic rats subcutaneously twice daily, it reduced pulmonary and splenic cfu counts significantly ($p < 0.01$) and their cfu counts were similar to those in WT rats (Fig. 2).

Histopathology of infection

When 3×10^6 cfu of the Kurono strain was given to the rats via the airborne route, larger granulomas were recognized in the lungs of the diabetic rats than in the WT controls (Fig. 3A). No Langerhans-like multinucleated giant cells were found in the granulomatous lesions. No necrotic lesions were present in these granulomas. The pulmonary granulomas merged with the surrounding granulomas over time, and foamy epithelioid macrophages were more prominent. Although no tubercle bacilli were noted in the pulmonary granulomas of WT rats, acid-fast tubercle bacilli were more prominent in the granulomas of diabetic rats (Fig. 3B). Small granulomas were recognized in the spleen and liver of diabetic rats. Conversely, the granulomas of WT rats were discrete and isolated (Fig. 3C).

The diabetic rats, which were given insulin twice daily after infection, were dissected histologically. The sizes of pulmonary granulomas in the insulin-treated diabetic rats were found to be reduced significantly (Fig. 3D).

In vitro effect of glucose on mycobacterial growth

Three different concentrations of glucose were added to *M. tuberculosis* in 7H9 liquid medium. Mycobacterial growth was concentration-dependent (Fig. 4), and maximal when 0.1% glucose was added to the tubercle bacilli ($p < 0.01$). Although 0.5% glucose also increased mycobacterial growth, the difference between 0.5% glucose and no addition was not statistically significant. Addition of 1% glucose did not induce growth of tubercle bacilli significantly (Fig. 4).

Real-time PCR

The data thus obtained were expressed as relative intensity (Fig. 5). In the lung tissues of non-infected KDP and WT rats, the expression levels of IFN-γ, TNF-α and IL-1β mRNA were very low (< 0.1 as relative intensity). The expression of pulmonary IFN-γ mRNA was higher at 7 weeks after infection in the infected diabetic rats than in control rats, the mRNA expression in the former being > 3 times that in the latter ($p < 0.01$). Pulmonary TNF-α mRNA expression in the infected diabetic rats was 4 times higher than in the infected control rats ($p < 0.01$). On the other

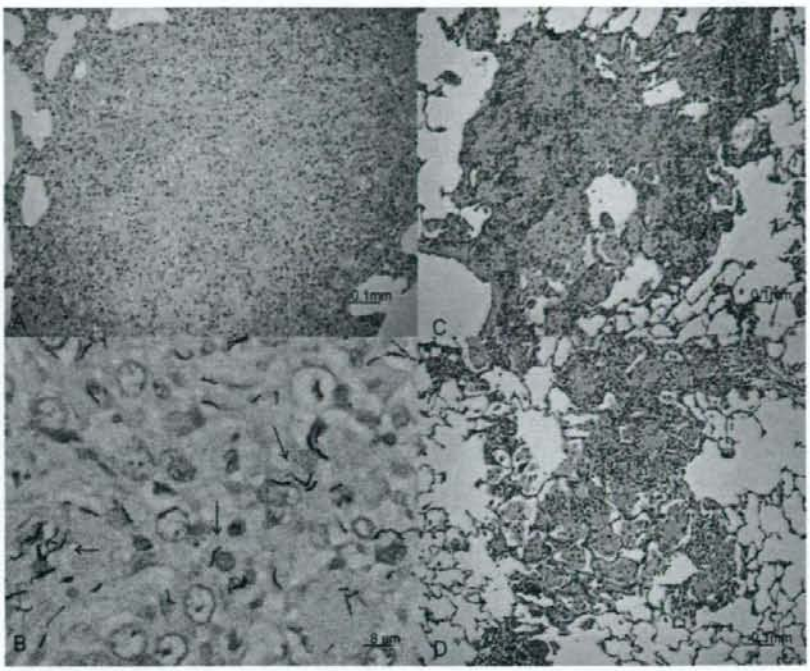

Fig. 3. Histopathology of the infected lung tissue.
Formalin-fixed sections were stained with hematoxylin and eosin (A, C and D) and Ziehl-Neelsen stain for acid-fast bacilli (→) (B).
(A) Pulmonary tissue from a diabetic type 1 (KDP) rat infected with the Kurono strain (7 weeks after infection)(magnification, × 100). (B) Pulmonary tissue from a KDP rat infected with the Kurono strain 7 weeks after infection (magnification, × 500) (C) Pulmonary tissue from a wild-type (WT) rat infected with the Kurono strain (7 weeks after infection)(magnification, × 100). (D) Pulmonary tissue from a KDP rat infected with the Kurono strain and treated with insulin twice daily (7 weeks after infection) (magnification, × 100). Larger granulomas were recognized in the lungs of KDP rats than in the WT controls (A). The sizes of pulmonary granulomas in the insulin-treated KDP rats were reduced significantly (D).

hand, the pattern of expression of pulmonary IL-1β mRNA was slightly different, and two times higher than in the infected controls.

Nitric oxide (NO) assay

NO levels in the culture supernatants of alveolar macrophages were determined using Griess reagent with reference to a standard $NaNO_2$ curve. The levels of NO produced by unstimulated alveolar macrophages from both KDP and WT rats were $< 20\,\mu$M. However, when the alveolar macrophages were stimulated overnight with the Kurono strain (multiplicity of infection=10), NO levels increased to $65 \pm 5\,\mu$M (control rats) and $25 \pm 2\,\mu$M (type 1 diabetic rats). The difference in NO secretion capacity between diabetic and WT rats was statistically significant ($p < 0.01$) (Table 1).

Discussion

In this study, large granulomas were induced in rats with type 1 diabetes after aerosol infection with *M. tuberculosis*. The number of cfu in lung and spleen tissues taken from the diabetic rats was significantly higher than that in WT control rats ($p < 0.01$). Similar findings were obtained when the experiments were repeated.

Although central necrosis was not recog-

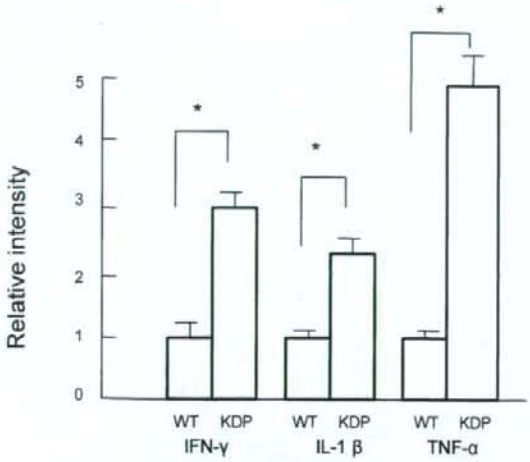

Fig. 4. Effect of glucose addition on *in vitro* mycobacterial growth.
$^*p < 0.01$ vs. WT rats. Glucose at 0.1%, 0.5% and 1% (w/v) was added to the *M. tuberculosis* Kurono strain in 7H9 medium, and the mixture was cultured for one week. Four weeks later, the number of cfu was determined.

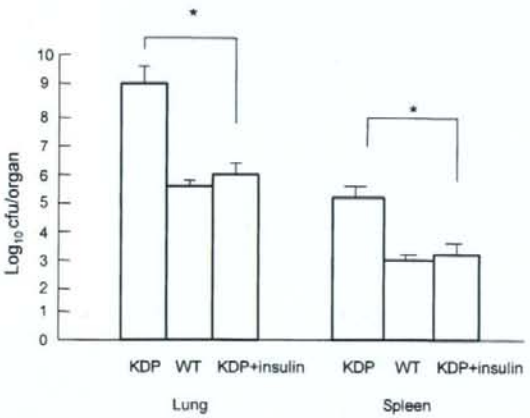

Fig. 5. *In vivo* expression profiles of pulmonary mRNA for IFN-γ, TNF-α or IL-1β in Kurono strain-infected rats. $^*p < 0.01$ vs. WT rats.
KDP, diabetic type 1; WT, wild-type. Pulmonary IFN-γ and TNF-α mRNA expression in the infected diabetic rats was significantly higher than in the infected control rats ($p < 0.01$)

TABLE 1. Nitric oxide (NO) production by alveolar macrophages stimulated with *M. tuberculosis* Kurono strain overnight.

Rat	Amount of NO produced (μM)	
	Unstimulated	Stimulated with Kurono strain
KDP	< 20	25 ± 2
WT	< 20	65 ± 5*

Alveolar macrophages (1×10^6/well) were plated in 96-well microculture plates in RPMI 1640 supplemented with 10% heat-inactivated fetal calf serum and stimulated with the Kurono strain overnight (multiplicity of infection=10). The NO concentration in the supernatants was determined by the Griess assay. Each value is mean±S.D. of the mean of three independent experiments. $^*p < 0.01$ vs. WT rats.

nized in the granulomas of diabetic rats, larger granulomas were induced in diabetic rats after infection with *M. tuberculosis*. Blood glucose levels ranged from 200 to 550 mg/dl. Impaired insulin secretion and hyperglycemia have been reported in diabetic rats (Komeda et al. 1998; Yokoi et al. 2003). As glucose induced mycobacterial growth significantly *in vitro*, a high glucose level in blood may be responsible for growth of *M. tuberculosis in vivo*. Impaired glucose tolerance may also be associated with active tuberculosis (Kimura et al. 1982; Oluboyo et al. 1990). The blood glucose level after *M. tuberculosis* infection did not increase significantly in diabetic and wild-type (WT) rats. Although clinical diabetes mellitus is frequently associated with hyperlipidemia and hypercholesterolemia (Powers 2008), blood lipid and cholesterol levels in diabetic rats were within the normal ranges. Hyperglycemia is common in patients with tuberculosis, and individuals who have no prior history of diabetes mellitus (DM) may present with glucose intolerance at the time of diagnosis. In a study of 506 patients with active pulmonary tuberculosis, nine had a history of DM, 25 were found to be newly diabetic, and 82 had impaired glucose tolerance (Mugusi et al. 1990). This suggests that, like other serious

infections, active tuberculosis is associated with hyperglycemia. Our laboratory findings have provided substantial evidence to support this clinical observation.

TNF-α, IFN-γ and IL-1β are important inflammatory cytokines. A few clinical studies have investigated serum cytokine levels in DM patients (Maltezos et al. 2002; Ozer et al. 2003). The highest serum IL-1α and IFN-γ levels were found in newly diagnosed type 1 DM patients without diabetic ketoacidosis. Expression of TNF-α, IFN-γ and IL-1β mRNA was relatively high at 7 weeks after infection, indicating that inflammatory changes in the lungs flare up, and may explain the large granulomas in type 1 diabetic rats.

Although no significant difference was noted in phagocytosis of tubercle bacilli by alveolar macrophages from diabetic type 1 and WT rats (data not shown), alveolar macrophages from the diabetic rats produced less NO than those from WT rats. NO is a well-known anti-tuberculous substance synthesized by inducible NO synthase in macrophages (Chan et al. 1992). Therefore, it is thought that alveolar macrophages from diabetic rats cannot be activated fully to produce NO upon stimulation with tubercle bacilli. Similar findings have been obtained in GK type 2 diabetic rats (Goto et al. 1976; Sugawara et al. 2004).

It is very important to measure the blood insulin level in diabetic rats because lack of insulin leads to hyperglycemia, which results in mycobacterial growth. When type 1 diabetic *M. tuberculosis*-infected rats were treated subcutaneously with insulin daily, the blood glucose level dropped from more than 550 mg/dl to ca. 200 mg/dl, and the number of cfu in the infected lung and spleen tissues was significantly decreased ($p < 0.01$). Thus, it is important to maintain the blood glucose level within the normal range to protect diabetic hosts from severe mycobacterial infection.

Diabetic type 1 rats are model animals of DM type 1. No studies have investigated the relationship between type 1 DM and mycobacterial infection using DM animal models. Non-obese diabetic (NOD) mice are a well-known model of type 1 DM and develop autoimmune diabetes, but there have been few studies of DM and mycobacterial infection. Diabetes-prone NOD mice are resistant to *M. avium* and the infection prevents autoimmune diabetes (Bras and Aguas 1996). In order to explain the mechanism of *M. avium*-induced resistance to insulin-dependent DM in NOD mice, the role of Fas and Th1 cells, and the increase in cytotoxicity of T cells have been highlighted (Martins and Aguas 1999). NOD mice are able to control *M. avium* infection, following a pattern similar to that observed in infected C3H mice. However, no report has indicated whether NOD mice can control *M. tuberculosis* infection. As the pathogenesis of DM in NOD mice is complicated, we chose the type 1 diabetic rat, a model established in 1998, to study the relationship between type 1 DM and tuberculosis. Unlike the findings observed in NOD mice, the diabetic rats displayed a different pattern in terms of histopathology and cfu count in lung and spleen tissues. Diabetic type 1 rats cannot control *M. tuberculosis* infection. Histopathology and cfu changes observed in the diabetic rats are similar to those in Goto Kakizaki (GK) rats. Much research has focused on diabetic type 1 rats in terms of the presence of insulin autoantibody, T cell function and islet cell antibody. We have already found that such rats have a high incidence of insulitis with lymphocyte infiltration and a good response to insulin treatment.

In conclusion, mycobacterial infection was studied in diabetic rats to investigate the basis for the high incidence of clinical tuberculosis in diabetic human patients. Our current findings clearly indicate that both GK type 2 diabetic and type 1 diabetic rats are highly susceptible to *M. tuberculosis* infection. Another important finding is that alveolar macrophages from KDP rats are not fully activated for killing of tubercle bacilli, unlike those from GK rats. Future studies should focus on the role of transcription factors in diabetic rats because NK-κB, STAT 4 and IRF-1 regulate the expression of interferons, IL-1 and TNF-α (Sugawara et al. 2003; Yamada et al. 2001; Yamada et al. 2002).

Acknowledgments

This study was supported in part by a Research Grant for Emerging and Re-emerging Infectious Diseases from the Ministry of Health, Welfare and Labour, Japan.

References

Banyai, A.L. (1931) Diabetes and pulmonary tuberculosis. *Am. Rev. Tuberc.*, **24**, 650-667.

Boucot, K.K., Dillon, E., Cooper, D. & Muer, P. (1952) Tuberculosis and diabetes. *Am. Rev. Tuberc.*, **65**, Suppl. 1, 1-50.

Bras, A. & Aguas, A.P. (1996) Diabetes-prone NOD mice are resistant to *Mycobacterium avium* and the infection prevents autoimmune disease. *Immunology*, **89**, 20-25.

Chan, J., Xing, Y., Magliozzo, R.S. & Bloom, B.R. (1992) Killing of virulent *Mycobacterium tuberculosis* by reactive nitrogen intermediates produced by activated murine macrophages. *J. Exp. Med.*, **175**, 1111-1122.

Garay, S.M. (2004) Pulmonary tuberculosis In Tuberculosis (ed. by Rom, W.N. and Garay, S.M.). p. 345. LWW, Philadelphia.

Goto, Y., Kakizaki, M. & Masaki, N. (1976) Production of spontaneous diabetic rats by repetition of selective breeding. *Tohoku J. Exp. Med.*, **119**, 85-90.

Green, S.J., Crawford, R.M., Hockmeyer, J.T., Meltzer, M.S. & Nacy, C.A. (1990) Leishmania major amastigotes initiate the L-arginine-dependent killing mechanism in IFN-γ stimulated macrophages by induction of tumor necrosis factor-α. *J. Immunol.*, **145**, 4290-4297.

Kim, S.J., Hong, Y.P., Lew, W.J., Yang, S.C. & Lee, E.G. (1995) Incidence of pulmonary tuberculosis among diabetics. *Tuber. Lung Dis.*, **76**, 529-533.

Kimura, K., Toyota, T., Kakizaki, M., Kudo, M., Takebe, K. & Goto, Y. (1982) Impaired insulin secretion in the spontaneous diabetic rats. *Tohoku J. Exp. Med.*, **137**, 453-459.

Komeda, K., Noda, M., Terao, K., Kuzuya, N., Kanazawa, M. & Kanazawa, Y. (1998) Establishment of two substrains, diabetes-prone and non-diabetic, from Long-Evans Tokushima lean (LETL) rats. *Endocr. J.*, **45**, 737-744.

Makino, S., Kunimoto, K., Muraoka, Y., Mizushima, Y., Katagiri, K. & Tochino, Y. (1976) Breeding of a non-obese, diabetic strain of mice. *Exp. Animals*, **29**, 1-13.

Maltezos, E., Papazoglou, D., Exiara, T., Papazoglou, L., Karathanasis, E., Christakidis, D. & Ktenidou-Kartali, S. (2002) Tumor necrosis factor-α levels in non-diabetic offspring of patients with type 2 diabetes mellitus. *J. Int. Med. Res.*, **30**, 576-583.

Martins, T.C. & Aguas, A.P. (1999) Mechanisms of *Mycobacterium avium*-induced resistance against insulin-dependent diabetes mellitus (IDDM) in non-obese diabetic (NOD) mice: role of Fas and Th1 cells. *Clin. Exp. Immunol.*, **115**, 248-254.

Mugusi, F., Swai, A.B.M., Alberti, K.G.M.M. & McLarty, D.G. (1990) Increased prevalence of diabetes mellitus in patients with pulmonary tuberculosis in Tanzania. *Tubercle*, **71**, 271-276.

Oluboyo, P.O. & Erasmus, R.T. (1990) The significance of glucose intolerance in pulmonary tuberculosis. *Tubercle*, **71**, 135-138.

Ozer, G., Teker, Z., Cetiner, S., Yilmaz, M., Topaloglu, A.K., Oneli-Mungan, N. & Yuksel, B. (2003) Serum IL-1, IL-2, TNF-α and IFN-γ levels of patients with type 1 diabetes mellitus and their siblings. *J. Pediatr. Endocrinol. Metab.*, **16**, 203-210.

Powers, A.C. (2008) Diabetes mellitus. In Harrison's principle of internal medicine (ed. by Fauci, A., Braunwald, E., Kasper, D., Hauser, S., Longo, D., Jameson, J. & Loscalzo, J.) p. 2275. McGraw-Hill, New York.

Root, H.F. (1934) The association of diabetes and tuberculosis. *N. Eng. J. Med.*, **210**, 1-13.

Sugawara, I., Yamada, H. & Mizuno, S. (2003) Relative importance of STAT 4 in murine tuberculosis. *J. Med. Microbiol.*, **52**, 29-34.

Sugawara, I., Yamada, H. & Mizuno, S. (2004) Pulmonary tuberculosis in spontaneously diabetic Goto Kakizaki rats. *Tohoku J. Exp. Med.*, **204**, 135-145.

Yamada, H., Mizuno, S., Reza-Gholizadeh, M. & Sugawara, I. (2001) Relative importance of NF-κB p50 in mycobacterial infection. *Infect. Immun.*, **69**, 7100-7105.

Yamada, H., Mizuno, S. & Sugawara, I. (2002) Interferon regulatory factor 1 in mycobacterial infection. *Microbiol. Immunol.*, **46**, 751-760.

Yamada, H., Udagawa, T., Mizuno, S., Hiramatsu, K. & Sugawara, I. (2005) Newly designed primer sets available for evaluating various cytokines and iNOS mRNA expression in guinea pig lung tissues by RT-PCR. *Exp. Anim.*, **54**, 163-172, 2005.

Yamada, H., Mizuno, S., Ross, A.C. & Sugawara, I. (2007) Retinoic acid therapy attenuates the severity of tuberculosis while altering lymphocyte and macrophage numbers and cytokine expression in rats infected with *Mycobacterium tuberculosis*. *J. Nutr.*, **137**, 2696-2700.

Yokoi, N., Komeda, K., Wang, H.Y., Yano, H., Kitada, K., Saitoh, Y., Seino, Y., Yasuda, K., Serikawa, T. & Seino, S. (2002) Cb1b is a major susceptibility gene for rat type 1 diabetes mellitus. *Nat. Genet.*, **31**, 391-394.

Yokoi, N., Namae, M., Fuse, M., Wang, H.Y., Hirata, T., Seino, S. & Komeda, K. (2003) Establishment and characterization of the Komeda diabetes-prone rat as a segregating inbred strain. *Exp. Anim.*, **52**, 295-301.

Journal of Medical Microbiology (2008), 57, 873–880 DOI 10.1099/jmm.0.47564-0

Promising loci of variable numbers of tandem repeats for typing Beijing family *Mycobacterium tuberculosis*

Yoshiro Murase, Satoshi Mitarai, Isamu Sugawara, Seiya Kato and Shinji Maeda

Research Institute of Tuberculosis, Japan Anti-Tuberculosis Association, 3-1-24 Matsuyama, Kiyose, Tokyo 204-8533, Japan

Correspondence
Shinji Maeda
maeda@jata.or.jp

We analysed the genotypes of 325 *Mycobacterium tuberculosis* clinical isolates obtained during 2002 throughout Japan. The genotyping methods included insertion sequence IS*6110* RFLP, spoligotyping and variable number of tandem repeat (VNTR) analyses. Clustered isolates revealed by IS*6110* RFLP analysis accounted for 18.5% (60/325) of the isolates. Beijing genotype tuberculosis (TB) accounted for 73.8% (240/325) of the isolates. Using VNTR, we analysed 35 loci, including 12 standard mycobacterial interspersed repetitive units and 4 exact tandem repeats. The discriminatory power of these 16 loci was low. Using VNTR analyses of the 35 loci, 12 loci (VNTRs 0424, 0960, 1955, 2074, 2163b, 2372, 2996, 3155, 3192, 3336, 4052 and 4156) were selected for the genotyping of Beijing genotype strains. Comparison of the discriminatory power of the 12-locus VNTR [Japan Anti-Tuberculosis Association (JATA)] to that of the 15-locus and 24-locus VNTRs proposed by Supply *et al.* (2006) showed that our established VNTR system was superior to the reported 15-locus VNTR and had almost equal discriminatory power to the 24-locus VNTR. This 12-locus VNTR (JATA) can therefore be used for TB genotyping in areas where Beijing family strains are dominant.

Received 8 August 2007
Accepted 13 March 2008

INTRODUCTION

RFLP analysis using insertion sequence IS*6110* is the gold standard of tuberculosis (TB) genotyping (Cave *et al.*, 1991; Kremer *et al.*, 1999; van Embden *et al.*, 1993). However, this RFLP analysis has many associated problems (Mostrom *et al.*, 2002).

Spoligotyping has been used throughout the world as a convenient and reproducible PCR-based method for genotyping (Kamerbeek *et al.*, 1997). Nevertheless, it provides little information related to Beijing family strains because spoligotypes of this genotype family show very little variation (Glynn *et al.*, 2002; Kremer *et al.*, 2004). In the countries of eastern Asia, the frequency of Beijing genotype TB is high. For that reason, spoligotyping is ineffective to discriminate unrelated isolates.

Analysis of variable number of tandem repeat (VNTR) loci is a promising PCR-based typing method. In VNTR analysis, some mini-satellite loci in the *Mycobacterium tuberculosis* genome are amplified using PCR; then their copy numbers are determined (Smittipat & Palittapongarnpim, 2000; Supply *et al.*, 2000). In fact, VNTR analysis with the standard 12 loci of mycobacterial interspersed repetitive units (MIRUs) has been used in the USA and Europe (Blackwood *et al.*, 2004; Mazars *et al.*, 2001). The Centers for Disease Control and Prevention (CDC) in the USA have adopted the standard 12-locus MIRU-VNTR for TB analyses (Cowan *et al.*, 2005; CDC, 2004). However, the discriminatory power of 12-locus MIRU-VNTR has been found to be insufficient (Supply *et al.*, 2006), which similarly applies to Beijing genotype TB analyses (Kam *et al.*, 2005; Kremer *et al.*, 2005; Nikolayevskyy *et al.*, 2006). Several reports have described other loci. Almost all corresponding loci have been described in the relevant literature (Iwamoto *et al.*, 2007; Kam *et al.*, 2006; Wada *et al.*, 2007).

It is noteworthy that a new 15-locus or 24-locus MIRU-VNTR method has been proposed in Europe (Oelemann *et al.*, 2007; Supply *et al.*, 2006). These new VNTR loci have had a distinct impact on genotyping of the Beijing family, but some large clusters remain (Iwamoto *et al.*, 2007). Therefore, several VNTR loci must be added to the reported 15-locus VNTR method for analyses of Beijing genotype strains (Yokoyama *et al.*, 2007).

For exploring the diversity of VNTR loci, we performed genotyping of IS*6110* RFLP, spoligotyping and 35-locus VNTR analysis using TB isolates from all over Japan. Based

Abbreviations: CDC, Centers for Disease Control and Prevention; ETR, exact tandem repeat; HGDI, Hunter–Gaston discriminatory index; JATA, Japan Anti-Tuberculosis Association; MIRU, mycobacterial interspersed repetitive unit; TB, tuberculosis; VNTR, variable number of tandem repeats.

47564 © 2008 SGM Printed in Great Britain

on these results, we propose a VNTR system that has the same discriminatory power as RFLP for analysis of a minimum number of loci in countries where the Beijing family has spread. Moreover, the results provide useful information for molecular epidemiological analyses of TB in regions where the Beijing genotype is dominant.

METHODS

***M. tuberculosis* isolates.** In all, 325 *M. tuberculosis* isolates, 3–10 strains per prefecture, were selected randomly from among 3122 isolates collected for a drug-resistance survey conducted in Japan in 2002 by the Tuberculosis Research Committee (RYOKEN). The isolates that we analysed had been originally considered as low cluster because the possibility of contact among patients was quite low. For comparing results of RFLP and VNTR analyses, 76 *M. tuberculosis* isolates were collected from 25 suspected epidemic outbreaks, along with epidemiological information. The epidemiologically linked 17 clusters (54 strains) showed the same RFLP pattern in each case. The 8 initially suspected TB patient clusters (22 strains) were found to be independent simultaneous occurrences: each strain had a different RFLP pattern. Mycobacterial genomic DNA was prepared from bacteria grown on Ogawa medium using an Isoplant kit (Nippon Gene).

Molecular typing methods. For this study, IS*6110* RFLP typing was performed according to a standardized protocol (van Embden *et al.*, 1993); band patterns were analysed using the BioNumerics software package (Applied Maths). In RFLP analysis, strains that have an identical band pattern were categorized as a cluster. Spoligotyping was also performed according to a standard protocol (Kamerbeek *et al.*, 1997). Sequences of primers used for amplification of 12 MIRU loci (MIRU-02, 04, 10, 16, 20, 23, 24, 26, 27, 31, 39 and 40), 4 exact tandem repeats (ETRs) (ETR-A, B, C and F) and 19 other loci (VNTRs 0424, 1612, 1895, 1955, 2074, 2163a, 2163b, 2347, 2372, 2401, 3155, 3171, 3232, 3336, 3690, 3820, 4052, 4120 and 4156) for VNTR were selected (Frothingham & Meeker-O'Connell, 1998; Iwamoto *et al.*, 2007; Roring *et al.*, 2002; Smittipat *et al.*, 2005; Supply *et al.*, 2001, 2006). The VNTR typing was performed using Ex *Taq* with GC PCR buffer I (Takara Bio). The PCR mixture was prepared in a 20 μl volume with 1 × GC PCR buffer I, 0.5 U Ex *Taq*, 200 μM each of four dNTPs, 0.5 μM each of the primer set and 10 ng template DNA. Then PCR was carried out for all loci under the following conditions: initial denaturation at 94 °C for 5 min, and then 35 cycles of 94 °C for 30 s, 63 °C for 30 s and 72 °C for 3 min, followed by a final extension at 72 °C for 7 min.

Estimation of molecular size of amplified DNA fragments. The sizes of the amplified DNA fragments were determined using a capillary array electrophoresis analysis system (*i*-Chip SV1210; Hitachi Electronics Engineering) (Sonehara *et al.*, 2006) or an ABI 3130 genetic analyser (Applied Biosystems) with the GeneMapper program (Applied Biosystems). The *i*-Chip was used to calibrate VNTR analysis and the genetic analyser was used to analyse the standard 12 loci MIRU (Iwamoto *et al.*, 2007; Supply *et al.*, 2001). Alternatively, the PCR products were analysed in a 2–2.5 % agarose gel. Their respective copy numbers were calculated from their size and assigned according to the number of repeats for each locus (Frothingham & Meeker-O'Connell, 1998; Kremer *et al.*, 2005; Skuce *et al.*, 2002; Supply *et al.*, 2001). The calculation accuracy was confirmed through analysis of *M. tuberculosis* H37Rv.

Allelic diversity and discrimination. The allelic diversity (h) at each VNTR locus was calculated using the index $h=1-\Sigma x_i^2$, where x_i is the frequency of the ith allele at the locus, as used in other studies (Kremer *et al.*, 2005; Sun *et al.*, 2004). The Hunter–Gaston discriminatory index (HGDI) was calculated in accordance with a method explained in another paper (Hunter & Gaston, 1988) to evaluate the combination of some VNTR loci.

Combinations of VNTR loci. For the following combination of VNTR loci, the HGDI were compared: 15-locus VNTR [Supply (15)] – VNTRs 0424, 0577, 0580, 0802, 0960, 1644, 1955, 2163b, 2165, 2401, 2996, 3192, 3690, 4052 and 4156; 24-locus VNTR [Supply (24)] – Supply (15) + VNTRs 0154, 2059, 2347, 2461, 2531, 2687, 3007, 3171 and 4348; 12-locus VNTR [Japan Anti-Tuberculosis Association (JATA) (12)] – VNTRs 0424, 0960, 1955, 2074, 2163b, 2372, 2996, 3155, 3192, 3336, 4052 and 4156.

RESULTS AND DISCUSSION

RFLP, spoligotyping and MIRU-VNTR analyses in Japan

From throughout Japan, 325 collected isolates were analysed using IS*6110* RFLP (Table 1). The percentage of clustered isolates was 18.5 % (60/325). In spoligotyping, 293 (90 %) isolates formed clusters; the maximum cluster size was 228. The largest cluster was composed of the Beijing genotype [70.2 % (228/325)]. Because the number of Beijing-like strains was 12 (Kremer *et al.*, 2004), the total of Beijing genotype strains used in this experiment was 240 (73.8 %). The Beijing family strains were confirmed to be dominant in Japan. The CDC in the USA has adopted the standard 12-locus MIRU-VNTR for TB analyses (Cowan *et al.*, 2005; CDC, 2004). We analysed the 325 TB isolates using 12-locus MIRU-VNTR and 16-locus VNTR (12 standard MIRU and 4 ETRs). There were only 89 unique types in the 12-locus MIRU-VNTR. The percentage of clustered isolates decreased from 72.6 % (12-MIRU-VNTR) to 62.8 % (16-locus VNTR) when the ETR loci were added to 12-locus MIRU analysis. Both rates of clustered isolates in VNTR analysis were higher than in RFLP (18.5 %). Furthermore, the HGDI showed that the discriminatory power of IS*6110* RFLP was the highest of all analyses used for this study: spoligotyping, 12-locus MIRU-VNTR and 16-locus VNTR.

An optimal 15-locus VNTR has been proposed by a consortium of European and American laboratories as a new worldwide standard method for discriminating TB genotypes using 52 different groups of related strains from different countries (Supply *et al.*, 2006). This VNTR method can discriminate in greater detail than the standard 12-locus MIRU-VNTR when the Beijing genotype of TB is analysed. However, it has been reported that the discriminatory power of 15-locus VNTR is insufficient for analysis of the Beijing genotype (Iwamoto *et al.*, 2007). The frequency of the Beijing family in Japan (80 % of total TB) (Yokoyama *et al.*, 2007) differs greatly from that in the USA (16 %) and European countries (4 %) (Filliol *et al.*, 2002). For that reason, new loci are necessary to analyse the Beijing family more effectively in Japan, Korea, China and other Asian countries.

Table 1. Comparison of the discriminatory power of IS*6110* RFLP, spoligotyping and VNTR analyses

Typing method	Total no. of type patterns	No. of unique types	No. of clusters	No. of clustered isolates (%)	Maximum no. of isolates in a cluster	HGDI*
IS*6110* RFLP	283	265	18	60 (18.5)	8	0.998
Spoligotyping	45	32	13	293 (90.2)	228	0.501
12-locus MIRU-VNTR	127	89	38	236 (72.6)	61	0.944
16-locus VNTR (12 MIRU and 4 ETRs)	165	121	44	204 (62.8)	44	0.967
8-locus VNTR (VNTRs 2163b, 4052, 3336, 1955, 4156, 2372, 0424 and 2074)	290	265	25	60 (18.5)	5	0.999
10-locus VNTR (8-locus VNTR + VNTRs 2996 and 3155)	297	276	21	49 (15.1)	4	0.999
12-locus VNTR (JATA) (10-locus VNTR + VNTRs 0960 and 3192)	302	284	18	41 (12.6)	4	0.999
15-locus VNTR (Supply)	291	269	22	56 (17.2)	6	0.999
24-locus VNTR (Supply)	303	287	16	38 (11.7)	4	0.999

*HGDI was calculated as described in Methods.

VNTR analyses of 19 loci

Different loci from those used for the USA or European countries must be examined when VNTR analysis is adopted for TB genotyping in Japan. Actually, VNTR analyses of 48 loci using 21 Beijing isolates have been reported (Smittipat *et al.*, 2005). Some loci that had high *h* for Beijing genotyping strains and other loci, such as Queen's University Belfast (QUB), were selected (Skuce *et al.*, 2002). In fact, 19 loci of 325 TB isolates were analysed using VNTR (Table 2). It was generally difficult to obtain the exact copy number using agarose gel electrophoresis in VNTR analysis when the molecular size of the PCR product was greater than 1 kb. More than 15 copies of repetitive units (larger than 1 kb) were detected at VNTRs 2163a, 2163b, 1895, 3232, 3336, 3820 and 4120. Only a few isolates had more than 15 copies of repetitive units at the loci of VNTRs 2163b, 1895 and 3336. However, for analyses of VNTRs 2163a, 3232, 3820 and 4120, more than 4 % of total isolates (18, 86, 50 and 14 strains, respectively) had 15 or more copies. For that reason, it was difficult to interpret the exact copy number. Furthermore, multiple PCR products were detected at the respective loci of VNTRs 2163b, 3232, 3336, 3820, 4120 and 4156. These had the potential to be unstable loci in VNTR analysis, and might be in the process of copy number change. Moreover, no PCR product was found in analyses of VNTRs 2163a, 2163b, 4052, 0424 and 2347.

From Japan, it was reported that VNTRs 3232, 3820 and 4120 are the hyper-variable loci (Iwamoto *et al.*, 2007; Wada *et al.*, 2007; Yokoyama *et al.*, 2007). More than 5 % of total isolates presented analytical problems (absence of PCR product, PCR products difficult to interpret or amplification of multiple alleles) at the loci of VNTRs 2163a, 3232, 3820 and 4120. Therefore, to obtain stable and precise VNTR results, these four loci were excluded from VNTR analyses of Beijing family strains.

New combination of VNTR loci for TB typing in Japan

The discriminatory power of each locus, based on the *h* values of all isolates, is presented in Table 3. The *h* of non-Beijing family strains was higher than that of the Beijing strain, except for VNTRs 0424, 2163b and 4156. These three loci were indispensable for distinction of the Beijing family.

One purpose of this study is to establish a new VNTR system with equal discriminatory power to that of RFLP using a minimum loci analysis in countries where the Beijing family is prevalent. Combinations of some loci, such as the top 8 loci (8-locus VNTR), top 10 loci (10-locus VNTR) or top 12 loci (12-locus VNTR), were compared to those of IS*6110* RFLP (Table 1) in terms of several characteristics, such as the number of unique isolates and clusters. In fact 8-locus VNTR had resolution performance that was equal to IS*6110* RFLP analysis in terms of the number of independent isolates and the rate of clustered isolates. Therefore, the 10-locus and 12-locus VNTRs were superior to IS*6110* RFLP. However, the quantities of clusters in VNTR analysis were comparable to those of RFLP only when 12-locus VNTR was used. Consequently, the primer set of the 12-locus VNTR (JATA) was ultimately selected for VNTR analysis in Japan.

Comparison of the discriminatory power of IS*6110* RFLP and VNTR analyses

A novel standard, optimized 15-locus and 24-locus VNTR primer sets (Supply *et al.*, 2006), was proposed recently (Table 3). The respective discriminatory powers of IS*6110* RFLP and VNTRs [15-locus (Supply) (Supply *et al.*, 2006), 24-locus (Supply) and 12-locus (JATA)] were compared using the percentage of clustered isolates (Fig. 1). The fraction of clustered isolates of 12-locus VNTR (JATA)

Table 2. The allelic profiles of 19 additional VNTR loci in 325 *M. tuberculosis* strains

VNTR locus	No. amplification	Multiple PCR products	Copy no. of repetitive unit(s)														
			0	1	2	3	4	5	6	7	8	9	10	11	12	13	14	15 and over*
2163a (QUB-11a)	5				10	27	5	12	27	10	30	103	51	15	5		7	18
2163b (QUB-11b)	3	1		6	29	56	35	35	35	75	39	6	1	2	1			1
3155 (QUB-15)					8	29	62	199	24	3								
1612 (QUB-23)							1		2	321	1							
4052 (QUB-26)	1		2	8	36	6	15	23	27	58	114	18	11	5	1			
1895				3	40	14	255	3	4		4							2
1955			4	29	41	141	71	31	2		1	1	3	1				
2074				18	83	179	39	6										
2372			1	22	78	156	58	7	3									
2401				6	114	4	200	1										
3232		1	1	8		2	23	25	5	8	6	17	18	27	36	22	40	86
3336		1	3	13	8	20	138	59	20	16	7	17	9	7	2	2	1	2
3820		1		2	9	10	32	9	6	9	12	14	8	31	51	44	37	50
4120		3	1	19	26	25	27	11	19	21	28	29	44	21	19	9	9	14
4156		1		12	96	75	131	10										
0424	1			15	72	61	171	4	1									
2347	1				13	8	302		1									
3171				1	2	319		3										
3690				6	17	248	19	21	7	7								

*The number of strains that had more than 15 copies in the locus are represented together in this column.

Table 3. The *h* values for each locus and details of the VNTR loci selected for the different VNTR analyses

No.	Locus	Alias	*h**			This study	Supply *et al.* (2006)†		12 MIRU +4 ETRs
			All isolates (*n*=325)	Beijing family (*n*=240)	Non-Beijing (*n*=85)	12 VNTR	24 VNTR	15 VNTR	
1	2163b	QUB 11b	0.855	0.815	0.802	×	×	×	
2	4052	QUB 26	0.812	0.764	0.860	×	×	×	
3	3336	VNTR 3336	0.768	0.642	0.894	×			
4	1955	Mtub 21	0.731	0.598	0.696	×	×	×	
5	4156	VNTR 4156	0.693	0.623	0.564	×	×	×	
6	2372	VNTR 2372	0.675	0.595	0.672	×			
7	0424	Mtub 04	0.635	0.468	0.425	×	×	×	
8	2074	Mtub 24	0.614	0.591	0.615	×			
9	2996	MIRU 26	0.591	0.314	0.667	×	×	×	×
10	3155	QUB 15	0.575	0.537	0.639	×			
11	0960	MIRU 10	0.546	0.431	0.704	×	×	×	×
12	3192	MIRU 31	0.545	0.270	0.416	×	×	×	×
13	2401	Mtub 30	0.498	0.379	0.463		×	×	
14	2165	ETR A	0.496	0.223	0.446		×	×	×
15	0802	MIRU 40	0.473	0.229	0.697		×	×	×
16	4348	MIRU 39	0.472	0.156	0.543		×		×
17	3690	Mtub 39	0.406	0.215	0.745		×	×	
18	1895	VNTR 1895	0.367	0.337	0.447				
19	3239	ETR F	0.358	0.237	0.575				×
20	1644	MIRU 16	0.345	0.258	0.502		×	×	×
21	2531	MIRU 23	0.336	0.158	0.555		×		×
22	0580	MIRU 4	0.189	0.049	0.484		×	×	×
23	2461	ETR B	0.151	0.017	0.447		×		×
24	0577	ETR C	0.134	0.057	0.317		×	×	×
25	2347	Mtub 29	0.129	0.095	0.214		×		
26	2059	MIRU 20	0.083	0.065	0.131		×		×
27	3007	MIRU 27	0.072	0.081	0.046		×		×
28	2687	MIRU 24	0.054	0	0.193		×		×
29	3171	Mtub 34	0.036	0.033	0.046		×		
30	1612	QUB 23	0.024	0.025	0.023				
31	0154	MIRU 2	0.018	0.008	0.046		×		×
32 (excluded)	3232	VNTR 3232	0.929	0.909	0.834				
33 (excluded)	4120	VNTR 4120	0.924	0.902	0.767				
34 (excluded)	3820	VNTR 3820	0.911	0.871	0.824				
35 (excluded)	2163a	QUB 11a	0.836	0.752	0.858				

**h* represents the allelic diversity of each locus, calculated as described in Methods.
†The combination of 15- and 24-locus VNTR analyses were reported by Supply *et al.* (2006).

(12.6 %) was superior to that of RFLP (18.5 %) and 15-locus VNTR (Supply) (17.2 %) in this experiment. The respective discriminatory capabilities of 15-locus and 24-locus VNTR (Supply) and 12-locus VNTR (JATA) were better than that of IS*6110* RFLP.

Our newly established 12-locus VNTR (JATA) typing method had almost equivalent discriminatory power to that of 24-locus VNTR (Supply) for TB genotyping, although it uses only 12 loci. In the 12-locus VNTR (JATA), 8 loci overlap with the 15-locus and 24-locus VNTRs (Supply): 4 loci (VNTRs 2074, 2372, 3155 and 3336) are independent. In the Supply VNTR typing method (Supply *et al.*, 2006), VNTR 3336 was discarded from the final selection for detection because of the following observations: it gave multiple PCR products, it did not give a PCR product and there was a lack of reproducibility between results obtained in independent laboratories. 'No PCR amplification' represents a characteristic typing datum; it indicates that the strain has different sequences in the primer binding site or has no such region. In addition, detection of a multiple PCR product might signify that a conversion of copy number is occurring at the locus, meaning that the genetic stability of such loci is not high.